AD-A084 051 ARMY ELECTRONICS RESEARCH AND DEVELOPMENT COMMAND FO--ETC F/G 9/5
DESIGN OF SILICON DIELECTRIC WAVEGUIDE LINE SCANNING ANTENNAS F--ETC(U)
AUG 78 K L KLOHN, R E HORN, H JACOBS

UNCLASSIFIED DELET-TR-78-19 NL

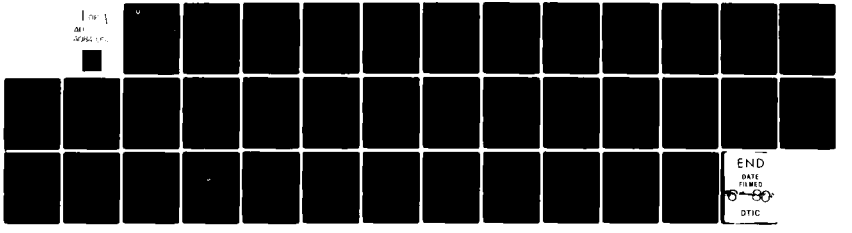

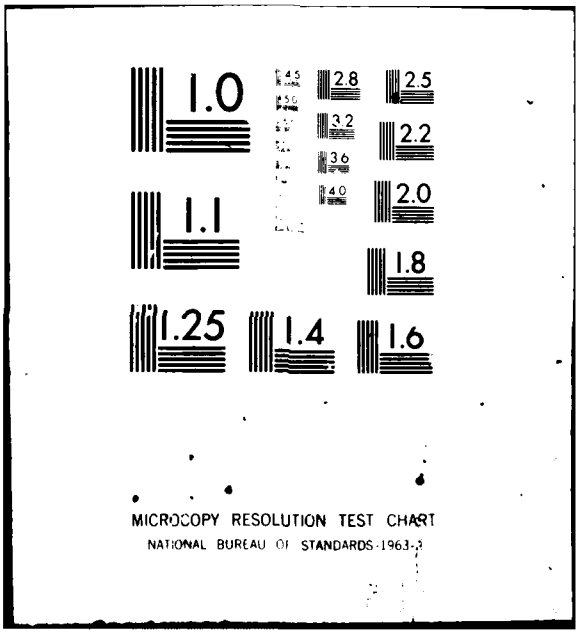
1.0
1.1
1.25
1.4
1.6
1.8
2.0
2.2
2.5
2.8
3.2
3.6
4.0
MICROCOPY RESOLUTION TEST CHART
NATIONAL BUREAU OF STANDARDS-1963-A

RESEARCH AND DEVELOPMENT TECHNICAL REPORT

DELET-TR-78-19

DESIGN OF SILICON DIELECTRIC WAVEGUIDE LINE SCANNING ANTENNAS FOR MILLIMETER WAVES

Kenneth L. Klohn
Robert E. Horn
Harold Jacobs
Elmer Freibergs

ELECTRONICS TECHNOLOGY & DEVICES LABORATORY

August 1978

ERADCOM

US ARMY ELECTRONICS RESEARCH & DEVELOPMENT COMMAND
FORT MONMOUTH, NEW JERSEY 07703

NOTICES

Disclaimers

The citation of trade names and names of manufacturers in this report is not to be construed as official Government indorsement or approval of commercial products or services referenced herein.

Disposition

Destroy this report when it is no longer needed. Do not return it to the originator.

SECURITY CLASSIFICATION OF THIS PAGE (When Data Entered)

REPORT DOCUMENTATION PAGE

READ INSTRUCTIONS BEFORE COMPLETING FORM

1. REPORT NUMBER: DELET-TR-78-19	2. GOVT ACCESSION NO.: AD-A084 051
3. RECIPIENT'S CATALOG NUMBER: Research and Development	
4. TITLE (and Subtitle): Design of Silicon Dielectric Waveguide Line Scanning Antennas for Millimeter Waves	5. TYPE OF REPORT & PERIOD COVERED: Technical Report
	6. PERFORMING ORG. REPORT NUMBER
7. AUTHOR(s): Kenneth L. Klohn, Robert E. Horn, Harold Jacobs, Elmer Freibergs	8. CONTRACT OR GRANT NUMBER(s): N/A
9. PERFORMING ORGANIZATION NAME AND ADDRESS: US Army Electronics Research & Development Command (ERADCOM) ATTN: DELET-MJ, Fort Monmouth, NJ 07703	10. PROGRAM ELEMENT, PROJECT, TASK AREA & WORK UNIT NUMBERS: 6944MD2158040 41
11. CONTROLLING OFFICE NAME AND ADDRESS	12. REPORT DATE: August 1978
	13. NUMBER OF PAGES: 32
14. MONITORING AGENCY NAME & ADDRESS (if different from Controlling Office)	15. SECURITY CLASS. (of this report): Unclassified
	15a. DECLASSIFICATION/DOWNGRADING SCHEDULE

16. DISTRIBUTION STATEMENT (of this Report)

Approved for Public Release: Distribution Unlimited

17. DISTRIBUTION STATEMENT (of the abstract entered in Block 20, if different from Report)

18. SUPPLEMENTARY NOTES

19. KEY WORDS (Continue on reverse side if necessary and identify by block number)

Dielectric Waveguide
Millimeter Waves
Frequency Scanning Antenna
Guide Wavelengths
Perturbation Spacing
Radiation Angle
Angular Scan

20. ABSTRACT (Continue on reverse side if necessary and identify by block number)

The design and experimental findings of a novel approach for a relatively simple, low cost, frequency scanning millimeter wave antenna are described. The antenna consists of a silicon dielectric rectangular rod with periodic metallic stripe perturbations on one side. The feasibility of electronically scanning through a range of angles by varying the frequency fed into the silicon rod is shown. Calculations were made to determine the allowable physical size of the silicon rod in order to maintain a single fundamental mode of operation and the effect which size variations and perturbation spacing have on the angle of

DD FORM 1 JAN 73 1473 EDITION OF 1 NOV 65 IS OBSOLETE UNCLASSIFIED

SECURITY CLASSIFICATION OF THIS PAGE (When Data Entered)

20. radiation and the range of angular scan for a given frequency shift. Efforts covered the frequency range 55 GHz to 100 GHz with specific points of interest at 60, 70 and 94 GHz. The results of experiments conducted are compared with the theoretical calculations.

CONTENTS

TABLES

DESIGN OF SILICON WAVEGUIDE FREQUENCY LINE SCANNING ANTENNAS FOR MILLIMETER WAVES

INTRODUCTION

Recent demands for a very high resolution radar in terminal homing for missiles and shells and for radar surveillance in general, have generated a need for developing new concepts in low-cost millimeter wave antennas. A means of providing electronic line scanning rather than mechanical scanning is very advantageous in order to be able to reduce the system complexity and high cost. It is especially important to eliminate the use of gimbals to mechanically scan an antenna since they are expensive and slow. This report describes the design and experimental findings of a novel approach for a side-looking electronic line scanner consisting of a dielectric (silicon) rectangular rod with periodic perturbations on one side. Angular scan in this approach is achieved by varying the frequency. The numerical values of the scan angles are a function of operating frequency, waveguide size (height and width) and perturbation spacing. Work was concentrated in the 55 GHz - 100 GHz frequency range.

The effect of varying the physical parameters will be shown in this report and comparisons made between theoretical calculations and experimental findings.

DESIGN CRITERIA

The key elements in the antenna design are operating frequency (in terms of λ_o), guide wavelength and perturbation spacing. These values determine the angle of radiating energy as seen in the following equation.[1,2]

$$\theta_n = \sin^{-1}\left(\frac{\lambda_o}{\lambda_g} + \frac{\lambda_o}{d}n\right) \; ; \; \left|\frac{\lambda_o}{\lambda_g} + \frac{\lambda_o}{d}n\right| \leq 1 \qquad [1]$$

where θ_n = beam angle from broadside (normal)

λ_o = free space wavelength

λ_g = guide wavelength

d = perturbation spacing

n = space harmonic; 0, $\pm$ 1, $\pm$ 2, ...

1. A. A. Oliner, Informal Communication, Class Notes from Polytechnical Institute of New York.
2. A. Hessel, "General Characteristics of Traveling-Wave Antennas", Antenna Theory Part 2, McGraw-Hill Book Company, New York, N. Y., 1969.

The operating frequency f_0 in a system is principally chosen by application requirements such as resolution, range and size of components. In a more practical sense, f_0 depends on the availability of millimeter wave power sources which are small, rugged, reliable and with sufficient power output for the intended application. Gunn and IMPATT diodes have been the primary solid state sources used to date. Preliminary work has been accomplished in incorporating these devices directly in dielectric waveguides at microwave frequencies where the guides are physically much larger than those studied in this report.[3-5] The bulk of the experimental work reported here was done near 60 GHz since sufficient test equipment and power sources were available. Some work was completed at 70 GHz and future experimental plans are aimed at 94 GHz.

The guide wavelength, for a given material and frequency, is determined by the physical size of the guide, i.e., width "a" and height "b". Since it is advantageous from a practical point of view to avoid as much multi-signal complexity as possible, single mode operation must be maintained in the propagation of energy in the waveguide with only a single beam of energy radiating from the antenna. Thus, the designs presented in this report which give the range (minimum and maximum) of guide sizes, allow only the E^y_{11} mode in the guide and the n = -1 space harmonic in the radiated energy.

Ideally, the waveguide should be kept as large as possible for any given frequency of operation as it eases fabrication problems and lessens the effect of size variations on the guide wavelength and scan angle. The maximum guide size is defined as that above which multiple mode operation is possible. The minimum guide size is defined as that below which the electric field becomes unguided. The maximum and minimum guide sizes were determined by calculating the propagation constants k_1, k_x and k_y (see Appendix A) using the transcendental equations formulated by Marcatili[6] and exactly solving them on a programmed calculator[7] using the relationship

$$k_z = \sqrt{k_1^2 - (k_x^2 + k_y^2)} \qquad [2]$$

which indicates that there is no propagation down the guide (z - direction) when $(k_x^2 + k_y^2)$ exceeds k_1^2. Figures 1, 2 and 3 were plotted for the fundamental E^y_{11} mode and the next two higher order modes E^y_{21} and E^y_{12} for the

3. M. M. Chrepta and H. Jacobs, "Millimeter-Wave Integrated Circuits", Microwave Journal, Vol 17, Nov 1974.
4. H. J. Kuno and Y. Chang, "Millimeter-Wave Integrated Circuits", U.S. Army Electronics Command Final Report No. ECOM-73-0279-F, June 1974.
5. Y. Chang and H. J. Kuno, "Millimeter-Wave Integrated Circuits", U.S. Army Electronics Command Final Report No. ECOM-74-0454-F, Oct 1975.
6. E. A. J. Marcatili, "Dielectric Rectangular Waveguide and Directional Coupler for Integrated Optics", Bell System Technical Journal, Vol. 48, No. 7, September 1969.
7. K. L. Klohn, J. F. Armata, Jr., and M. M. Chrepta, "Transverse Propagation Constants in Dielectric Waveguides", R&D Technical Report ECOM-4242, U.S. Army Electronics Command, Fort Monmouth, N. J., August 1974.

operating frequencies 60, 70 and 94 GHz. These plots show that the EY_{12} mode is the limiting mode for maximum guide size if a unity aspect ratio (a=b) is to be maintained. However, since k_x is independent of the guide height, the guide width could be made somewhat larger than the guide height; the limiting value being the cut-off point (size below which the mode will not propagate) for the E^y_{21} mode. The figures also indicate that λ_1, the wavelength in an infinite medium 1 (silicon in this case), can be used as a good first order approximation for the maximum allowed guide size and $\lambda_1/2$ as the minimum guide size. The equation for λ_1 is

$$\lambda_1 = 2\pi n_1 / \lambda_o \qquad [3]$$

where n_1 = index of refraction for medium 1

The figures for maximum and minimum guide size, both exact and approximate values, are listed in Table I.

TABLE I

MINIMUM AND MAXIMUM WAVEGUIDE SIZES FOR FUNDAMENTAL MODE E^y_{11}

FREQUENCY (GHz)	GUIDE SIZE (mm)			
	MIN	$\lambda_1/2$	MAX	$\lambda 1$
60	0.775	0.722	1.4	1.443
70	0.67	0.619	1.2	1.237
94	0.50	0.416	0.9	0.921

For any given waveguide size, the guide wavelength is also a function of operating frequency. Figure 4 illustrates how the guide wavelength varies with frequency for a silicon guide, a=b=0.9 mm (maximum guide size for single mode operation at 94 GHz.) As the operating frequency falls below the design frequency, λ_g increases rapidly. The λ_g (approximate) curve shown in the figure was obtained by using the following simplifying assumptions (See Appendix A).

$$(k_x A_{3,5}/\pi)^2 << 1 \quad \text{and} \quad (k_y A_{2,4}/\pi)^2 << 1 \qquad [4]$$

and then solving the transcendental equations in closed form. Table II shows the difference between λ_g (exact) and λ_g (approximate).

TABLE II

COMPARISON OF EXACT AND APPROXIMATE VALUES FOR GUIDE WAVELENGTH

FREQUENCY (GHz)	EXACT(mm)	APPROX(mm)	$\Delta\lambda g$(mm)	% DIFFERENCE
60	3.431	3.900	0.469	13.7
70	2.069	2.125	0.056	2.7
80	1.552	1.568	0.016	1.0
90	1.262	1.269	0.007	0.6

At frequencies above 80 GHz, $\Delta\lambda g$ becomes relatively insignificant. The variation in guide wavelength when "a" and "b" are changed but kept equal to each other, is shown in Figure 5. The smaller the guide size, the larger λ_g will be; a 10% change in guide dimensions changes λ_g approximately 5%. It will be illustrated later in this report how the changes in λ_g indicated in Figures 4 and 5, affect the angle of radiation from periodic radiating elements. Once the physical dimensions of the dielectric guide are chosen for a given frequency (In Fig. 1 a=b=1.4 mm is obtained as the maximum guide size for 60 GHz) the guide wavelength will be fixed for this frequency.

The only remaining variable to choose in Equation [1] for a given space harmonic (n = -1 in our case), is the perturbation spacing d. To obtain broadside radiation at a given frequency, d must be chosen equal to the guide wavelength at that frequency, thereby reducing θ_n to zero degrees. Actually it is nearly impossible to match d= λ_g exactly, therefore, the frequency at which $\theta_n = 0^o$ will be slightly different than the one designed to be zero.

LINE SCAN ANGLE

Figures 6, 7 and 8 give the angular scan that is theoretically possible (calculated from Equation [1]) by varying the operating frequency $f_o \pm 4$ GHz from the design frequency. A new set of propagation constants was calculated for each design frequency in order to determine the corresponding guide wavelength. It should be noted that the degrees of angular scan per GHz of frequency change decreases as the design frequency increases; 4.1^o/GHz at 60 GHz, 3.5^o/GHz at 70 GHz, and 2.5^o/GHz at 94 GHz. In addition, for frequencies above the design frequency, higher modes propagating in the guide is a possibility. Calculations indicated that radiation angles are very sensitive to changes or errors in λ_g. Experiments conducted to measure λ_g as a function of frequency, indicated that the measured values always exceeded the calculated values.[8]

8. H. Jacobs, G. Novick, C. M. LoCasio and M. M. Chrepta, "Measurement of Guide Wavelength in Rectangular Dielectric Waveguide", IEEE Transactions Microwave Theory and Techniques, Vol MTT-24, No 11, November 1976.

Figure 9 illustrates the effect on the radiation angle if λ_g is either + 10% from the calculated value while the perturbation spacing is kept approximately equal to the calculated λ_g value. Over the frequency range examined, the scan angles for λ_g-10% averaged $\sim 18^o$ higher and for λ_g + 10%, $\sim 14^o$ lower than the angles calculated for λ_g.

As previously mentioned, if the perturbation spacing is made equal to λ_g the radiation will be normal to the waveguide at the design frequency. The entire range of angular scan however, can be shifted more positive or negative by changing the spacing of the perturbations. (See Figure 10.) Closer spacing shifts the angle more negatively and conversely, increased spacing shifts the angle more positively. The slope, Δ degrees/Δfrequency, remains essentially constant. For each 0.1 mm change in d, the radiation angle changes approximately 8^o.

The range of scan angle, i.e., slope of the radiation angle curves, may be deliberately altered by changing the waveguide dimensions. As long as the dimensions remain between the minimum and maximum values, the energy will be guided and no higher modes will appear. (See Figure 11.) Smaller guide dimensions increase the slope, thereby increasing the scan range for a given Δf_o. In each case, the perturbation spacing was adjusted to match λ_g as close as practical. The curve for a=b=1.4 mm, crosses $\theta=0^o$ at 59 GHz rather than 60 GHz because the perturbation spacing does not match λ_g as well as for a=b=0.9 mm and a=b=1.0 mm. The results are tabulated in Table III.

TABLE III

ANGULAR SCAN FOR VARIOUS SIZE GUIDES (Δf_o = 8 GHz)

GUIDE SIZE a=b	PERTURBATION SPACING, d	RANGE OF ANGULAR SCAN
0.9 mm	3.4 mm	56^o
1.0	2.6	43^o
1.4	1.9	33^o

A variation of guide size and/or perturbation spacing to adjust the scan range could be used. Precautions should be taken to avoid multi-moding which would add to the complexity of the system by producing more than one radiating beam.

EXPERIMENTAL RESULTS

The objectives of the following experiments were to determine if a silicon waveguide with surface perturbations was an effective radiating structure; if the radiated beam was narrow in the y-z plane; and if the beam was steerable as a function of frequency.

Numerous silicon waveguides were fabricated with various cross-sectional dimensions and lengths to determine their effect on the radiation angle and range of angular scan.

The silicon waveguides, examined in this report, had dimensions of 0.969 mm x 1.071 mm x 10 cm for silicon waveguide #7 and 0.92 mm x 0.91 mm x 7 cm for silicon waveguide #2.

A series of perturbations (grating structures) on the silicon waveguide are required to provide a radiating surface. A grating structure, with grooves in a dielectric strip, used in a leaky wave antenna have been reported by Itoh.[9] The radiating structures covered in the following discussion uses metal perturbations on the top of a rectangular silicon rod. The perturbations consisted of 16 to 22 rectangular copper foil stripes with dimensions of 0.3 mm x 1 mm. The stripes were cemented to the top of the silicon to provide the perturbation structure. The distance from leading-edge-to-leading-edge of each metal stripe was set to an experimentally measured silicon waveguide wavelength λ_g as measured on an unperturbed silicon waveguide and checked with calculations using the Marcatili equations. The guide wavelength was measured using a test setup (see Figure 12) without perturbing stripes on the silicon waveguide and without the radiation angle test fixture. A flanged metal waveguide horn (terminated in a diode detector) was placed at a distance of less than 1 mm above the upper silicon surface in the near field of the propagated wave. The standing wave pattern on the silicon, produced by reflections due to an imperfect load, was then detected. The positions of the maxima points were determined using a calibrated micrometer (moveable in the z direction.) To obtain the average distance between maxima points, a large number of V_{max} measurements were made along the surface down the length of the guide.

The perturbation copper stripe spacing d was set equal to the measured λ_g. The perturbations covered a length of 4 cm using 16 stripes on the silicon waveguide. The silicon waveguide was then coupled to two adjoining metal waveguide sections using thin copper-foil end plates with 1 mm x 1 mm center openings (see Figure 13). The copper end plates provided the support for coupling the metal waveguide to the silicon waveguide by positioning the silicon in the center of the metal. The pointed silicon waveguide extended about 1 cm into each of the two matching metal waveguide sections. In addition, the copper end plates provided a shield to prevent radiation from the metal waveguide into the air surrounding the silicon guide.

With the silicon waveguide mounted in the test holder, (see Figure 13) the test setup (Figure 12) was subsequently assembled and the radiation pattern from the silicon waveguide was measured. The test setup was used to monitor forward power (P_f), reflected power (P_r), transmitted power (P_t), frequency (f_0), relative radiated power (P_{rad}) and radiation angle (θ). The flanged pickup horn (terminated in a diode detector and sensitive amplifier), was positioned at a distance of 20 cm from the exact center of the perturbation stripes. The flanged horn could then be positioned at any angle θ from -85^0 to $+ 85^0$ in the y-z plane on a calibrated test fixture. End absorbers (carbon compound material) were positioned directly over each end

9. T. Itoh, "Leaky-Wave Antenna and Band Reject Filter for Millimeter-Wave Integrated Circuits", 1977 IEEE MTT-S International Microwave Symposium Digest, Jun 21-23, 1977, pp 538-541.

at the dielectric-to-metal-waveguide transitions (Figure 13) to prevent radiation leakage. The test setup used an IMPATT diode oscillator variable in frequency from 55 to 63 GHz and a PIN diode modulator with a positive square wave modulation of about 1 kHz applied from the source. The PIN diode provided an amplitude modulated output down the waveguide which subsequently radiated out of the silicon surface.

Two experimental waveguides were prepared as indicated in Table IV.

TABLE IV

PHYSICAL CHARACTERISTICS OF EXPERIMENTAL WAVEGUIDES

Silicon Waveguide	$\bar{a}$ width (Ave) mm	$\bar{b}$ height (Ave) mm	l length (overall) mm	n Number of Stripes	l_1 Length of Exposed Silicon mm	$\bar{d}$ Spacing between perturbation mm
# 2	0.91	0.92	7	16	5.4	0.25
# 7	0.969	1.071	10	22	8	0.18

The radiation pattern of silicon waveguide #7, at a test frequency of 58.49 GHz is shown in Figure 14a. The polar plot of relative detected power shows a negative angle $\theta = 54^{o}$ at the peak radiation point. The half-power points occur at 50 units (power plot) indicating a beamwidth of about 4^{o}. The plot was obtained by arbitrarily setting the maximum value of radiated power at 100 units on the ac amplifier meter and moving the pickup horn through an angle $\pm\ \theta$ on either side of the peak to obtain the detected power plot.

Figure 14b shows a typical cross-sectional radiation pattern in a plane r-ϕ which is perpendicular to the plane shown in Figure 14a. Thus, the three dimensional radiation pattern is narrow in the y-z plane and wide (fan shaped) in the r-ϕ plane. Point-by-point frequency tests on silicon waveguide #7 yielded the relationship between radiation angle θ and frequency. (See Figure 15.) For frequencies between 57 GHz and 65 GHz, the center of the radiated beam (θ_{max}) varied from -68^{o} to -7^{o}, a change of 7.5^{o}/GHz. The above measurements were based on operation in the fundamental waveguide E^{y}_{11} mode. The 1 mm by 1 mm guide dimensions do not allow higher modes to propagate.

Using Equation [1], λ_g can be estimated by measuring θ, the angle of radiation and d the perturbation spacing. The wavelength in air λ_o can be calculated from the measurement of frequency.

In Figure 16, a plot was made of the guide wavelength λ_g for silicon waveguide #2 which had dimensions 0.92 mm by 0.91 mm with $d \cong 2.5$ mm. The experimental λ_g is plotted from 61 to 66 GHz and is greater than the theoretical values (exact and approximate) obtained from the Marcatili equations.

The radiation angle θ (experimental and theoretical) vs frequency for silicon waveguide #2, is plotted in Figure 17a. A comparison of the experimental and theoretical angles (see Figure 17a) indicates that the experimental values are more negative than the theory. A comparison was also made in Figure 17b between the experimental measurements and theoretical calculations for silicon waveguide #7 with d = 1.8 mm. It is again noted that the experimental points (circled points) occur at a more negative angle θ than the theoretical curve, indicating that experimental λ_g is, in both cases, greater than the theoretical λ_g. This agrees with previous direct measurements of λ_g using probe techniques.

SUMMARY AND CONCLUSIONS

Line scanning antennas were designed at millimeter wave frequencies (55 GHz to 100 GHz) with confirming experiments using rectangular silicon waveguides with metal stripe perturbations. Experiments indicated that a narrow beam of radiated power can be deliberately scanned through a range of angles by altering the input frequency. Using Marcatili's basic equations, the maximum and minimum waveguide sizes were determined allowing only the fundamental E^y_{11} mode for 60, 70 and 94 GHz. The key parameters of Equation [1], guide wavelength λ_g and perturbation spacing d, were theoretically and experimentally varied to determine their effect and criticality to the angle of radiation and range of angular scan. The theoretical results indicate that the radiation angle is very sensitive to changes in λ_g; a 10% change causing an angular shift of approximately 15 to 20°. The guide wavelength, in turn, for a given material and frequency, is determined by the physical dimensions of the guide; width a and height b.

Small changes in the spacing of the perturbations can also cause significant angular changes; 8° shifts for each 0.1 mm change in d. These results gave an indication as to how an antenna could be designed to cover a desired range of angular scan by altering the physical dimensions of the guide and/or changing the perturbation spacing.

Experiments were carried out to verify the calculated values of λ_g by detecting the standing wave pattern and measuring the distance between maxima, $\lambda_g/2$. In addition, λ_g was determined from Equation [1] using experimentally measured angles of radiation. The experimental λ_g values are plotted in Figure 16 and compared to the theoretical calculations. Both of the experimental techniques for determining λ_g indicate larger numerical values for any given frequency than theory would predict[8, 10]. Both techniques, however, show that the difference between experiment and theory decreases as the frequency increases. The experimentally measured radiation angles for silicon waveguides #2 ($\bar{a}$ = 0.91 mm, $\bar{b}$ = 0.92 mm, $\bar{d}$ = 2.5 mm) and #7 ($\bar{a}$ = 0.97 mm, $\bar{b}$ = 1.07 mm, $\bar{d}$ = 1.8 mm) are plotted in Figures 17a and 17b, respectively. These angles are compared with theoretically calculated angles for guide sizes and perturbation spacings closely matching the average values.

10. H. Jacobs, G. Novick, C. M. LoCasio, "Probe Measurements of Guide Wavelength in Rectangular Silicon Dielectric Waveguide", 1977 IEEE MTT-S International Microwave Symposium Digest, Jun 21-23, 1977, pp 118-120.

The values for a, b and d used in the theoretical calculations, bracket the actual variation in parameters for the experimental waveguide antennas. The results show that the observed radiation angles fall within the theoretical limits and agreement is good, especially since, the angle θ_n is very sensitive to changes in λ_g (and therefore a and b) and d.

The feasibility has been shown of electronically scanning through a range of angles by varying the frequency fed into a relatively simple antenna structure consisting of a rectangular silicon rod with copper stripes (perturbations) attached to the upper surface and how the range of scan can be altered by changing the physical dimensions of the guide and the spacing between perturbations.

ACKNOWLEDGMENT

This work was supported by the Ballistic Missile Defense Advanced Technology Center, Huntsville, Alabama, and by the U. S. Army In-House Laboratory Independent Research Program, Fort Monmouth, New Jersey. The authors would like to thank Fan King of the Ballistic Missile Defense Advanced Technology Center for his helpful discussions and encouragement.

REFERENCES

(1) A. A. Oliner, Informal Communication, Class Notes from Polytechnical Institute of New York

(2) A. Hessel, "General Characteristics of Traveling-Wave Antennas", Antenna Theory Part 2, McGraw-Hill Book Company, New York, N.Y., 1969

(3) M. M. Chrepta and H. Jacobs, "Millimeter-Wave Integrated Circuits", Microwave Journal, Vol 17, Nov 1974

(4) H. J. Kuno and Y. Chang, "Millimeter-Wave Integrated Circuits", U.S. Army Electronics Command Final Report No. ECOM-73-0279-F, June 1974

(5) Y. Chang and H. J. Kuno, "Millimeter-Wave Integrated Circuits", U.S. Army Electronics Command Final Report No. ECOM-74-0454-F, Oct 1975

(6) E. A. J. Marcatili, "Dielectric Rectangular Waveguide and Directional Coupler for Integrated Optics", Bell System Technical Journal, Vol 48, No. 7, September 1969

(7) K. L. Klohn, J. F. Armata, Jr., and M. M. Chrepta, "Transverse Propagation Constants in Dielectric Waveguides", R&D Technical Report ECOM-4242, U. S. Army Electronics Command, Fort Monmouth, N.J., August 1974

(8) H. Jacobs, G. Novick, C. M. LoCasio and M. M. Chrepta, "Measurement of Guide Wavelength in Rectangular Dielectric Waveguide", IEEE Transactions Microwave Theory and Techniques, Vol MTT-24, No 11, November 1976

(9) T. Itoh, "Leaky-Wave Antenna and Band Reject Filter for Millimeter-Wave Integrated Circuits", 1977 IEEE MTT-S International Microwave Symposium Digest, Jun 21-23, 1977, pp 538-541

(10) H. Jacobs, G. Novick, C. M. LoCasio, "Probe Measurements of Guide Wavelength in Rectangular Silicon Dielectric Waveguide", 1977 IEEE MTT-S International Microwave Symposium Digest, Jun 21-23, 1977, pp 118-120

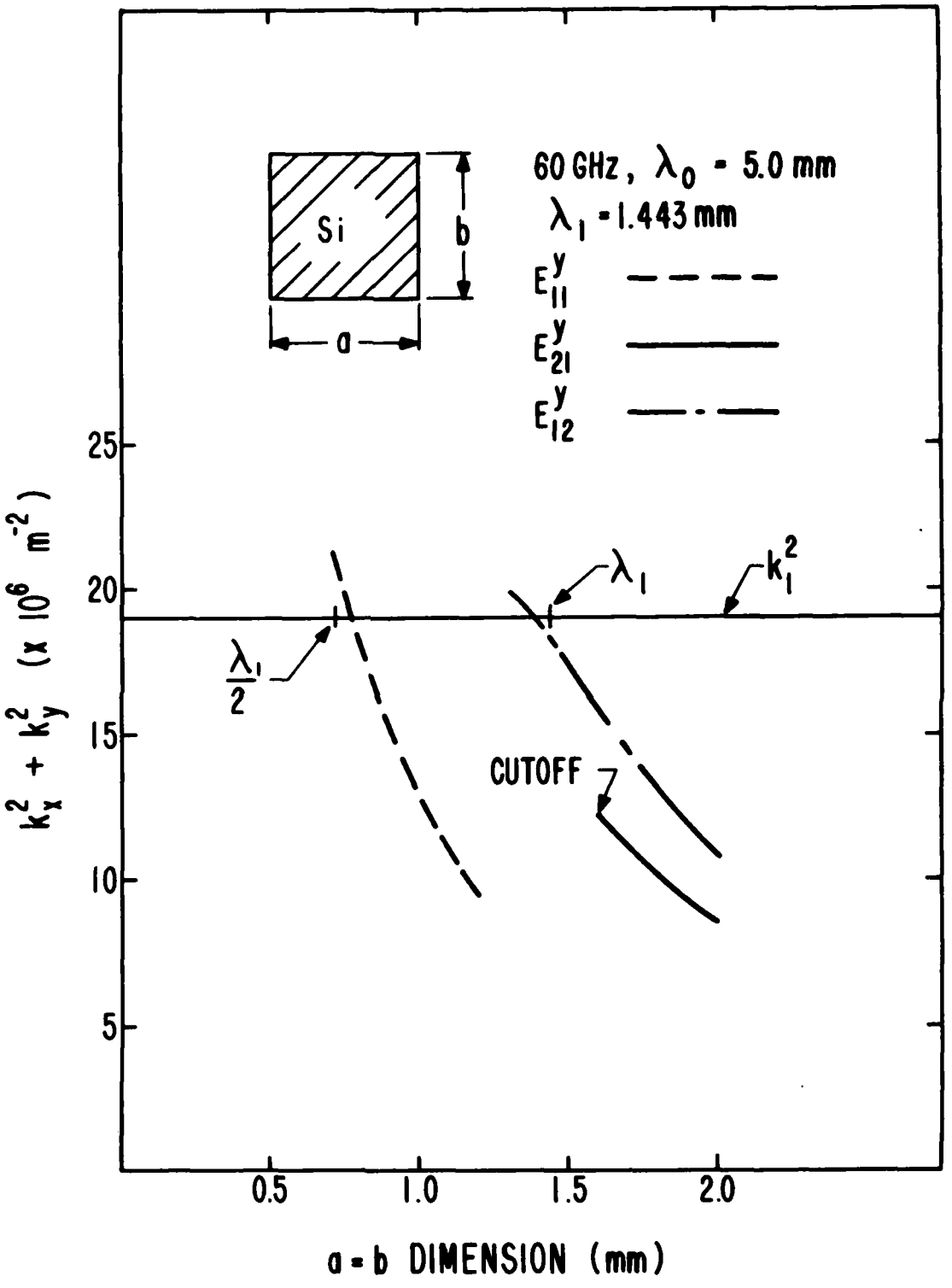

Figure 1 Minimum and Maximum Waveguide Dimensions, 60 GHz

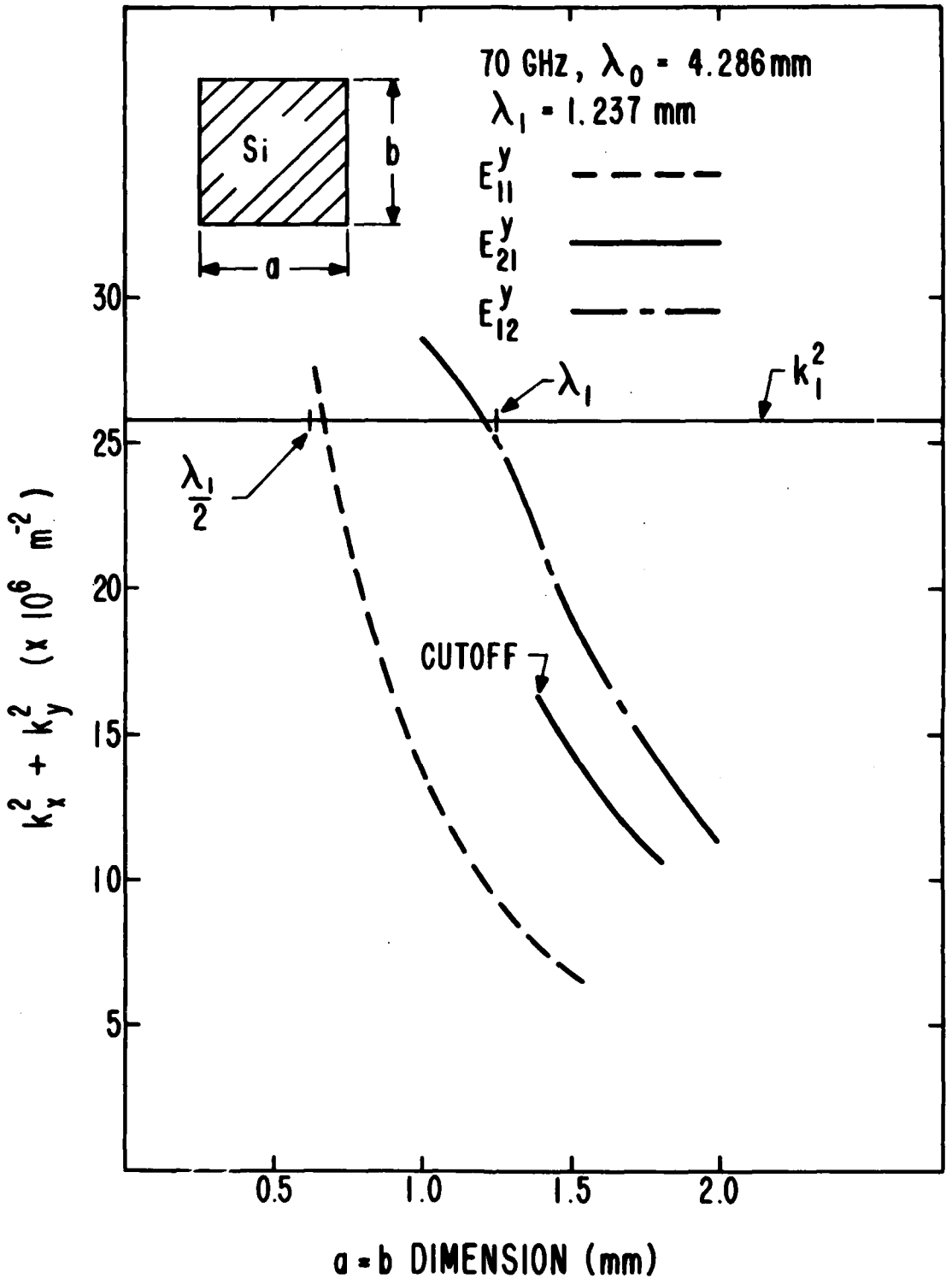

Figure 2 Minimum and Maximum Waveguide Dimensions, 70 GHz

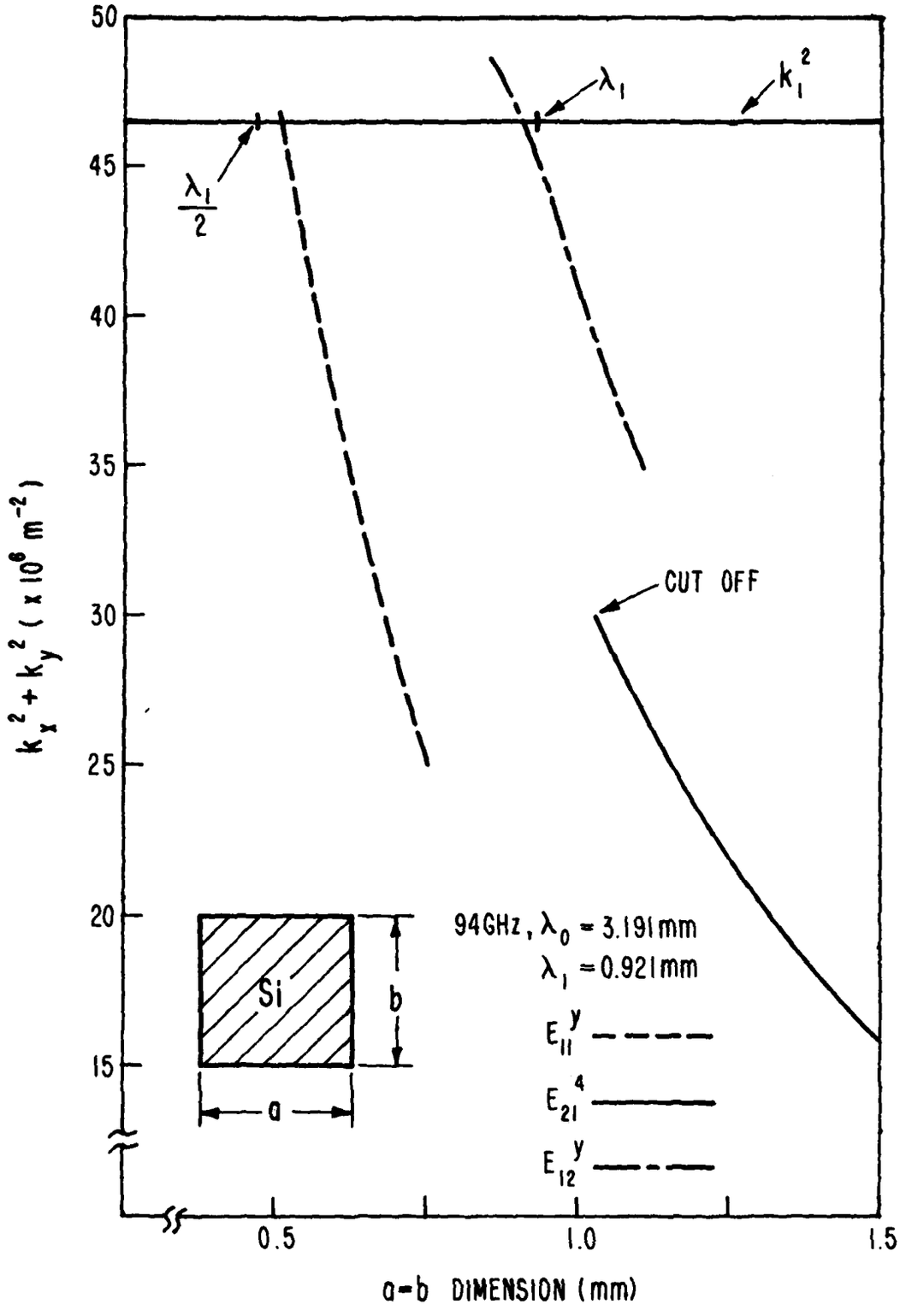

Figure 3 Minimum and Maximum Waveguide Dimensions, 94 GHz

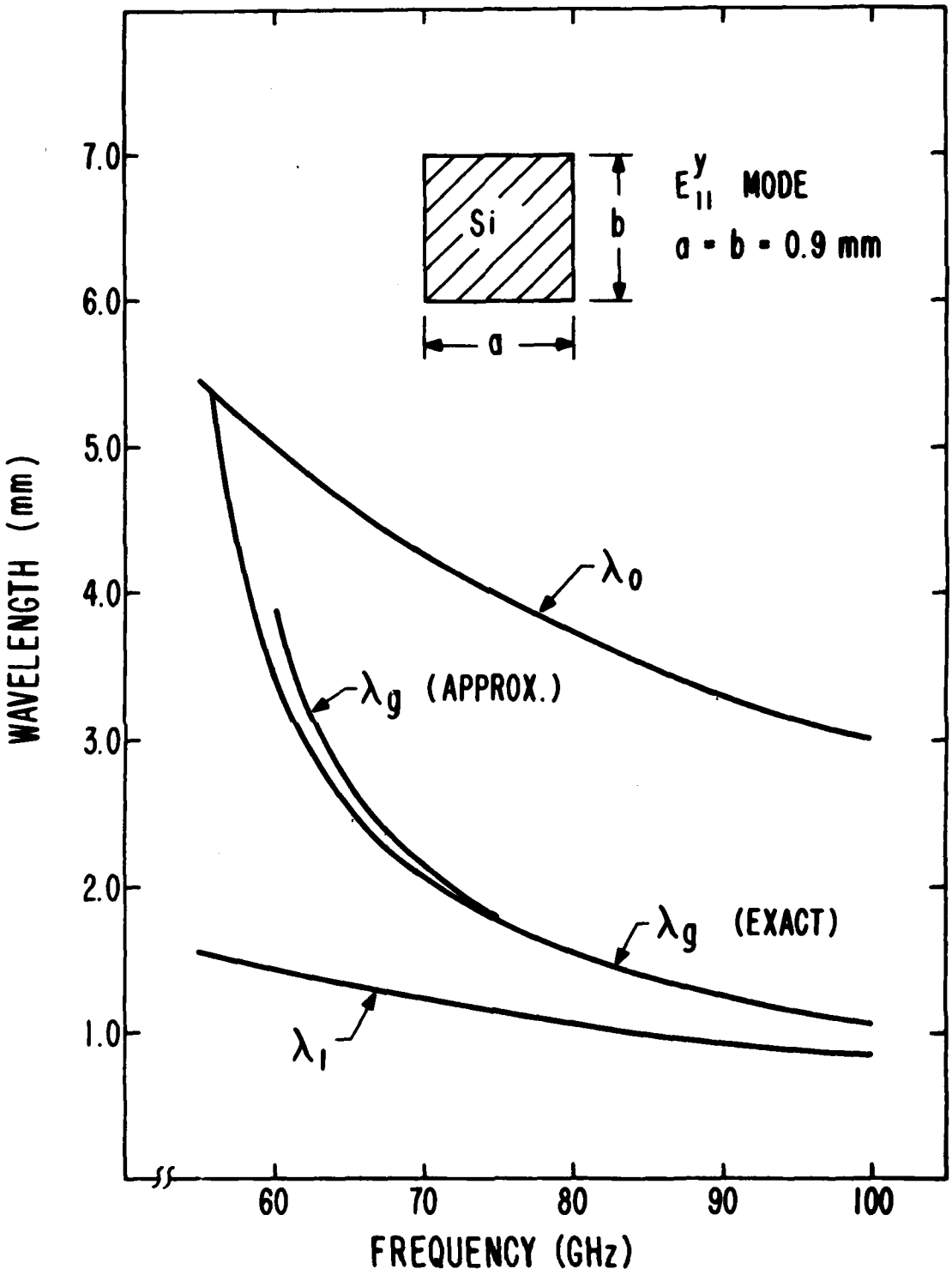

Figure 4 Variation of Wavelength with Frequency

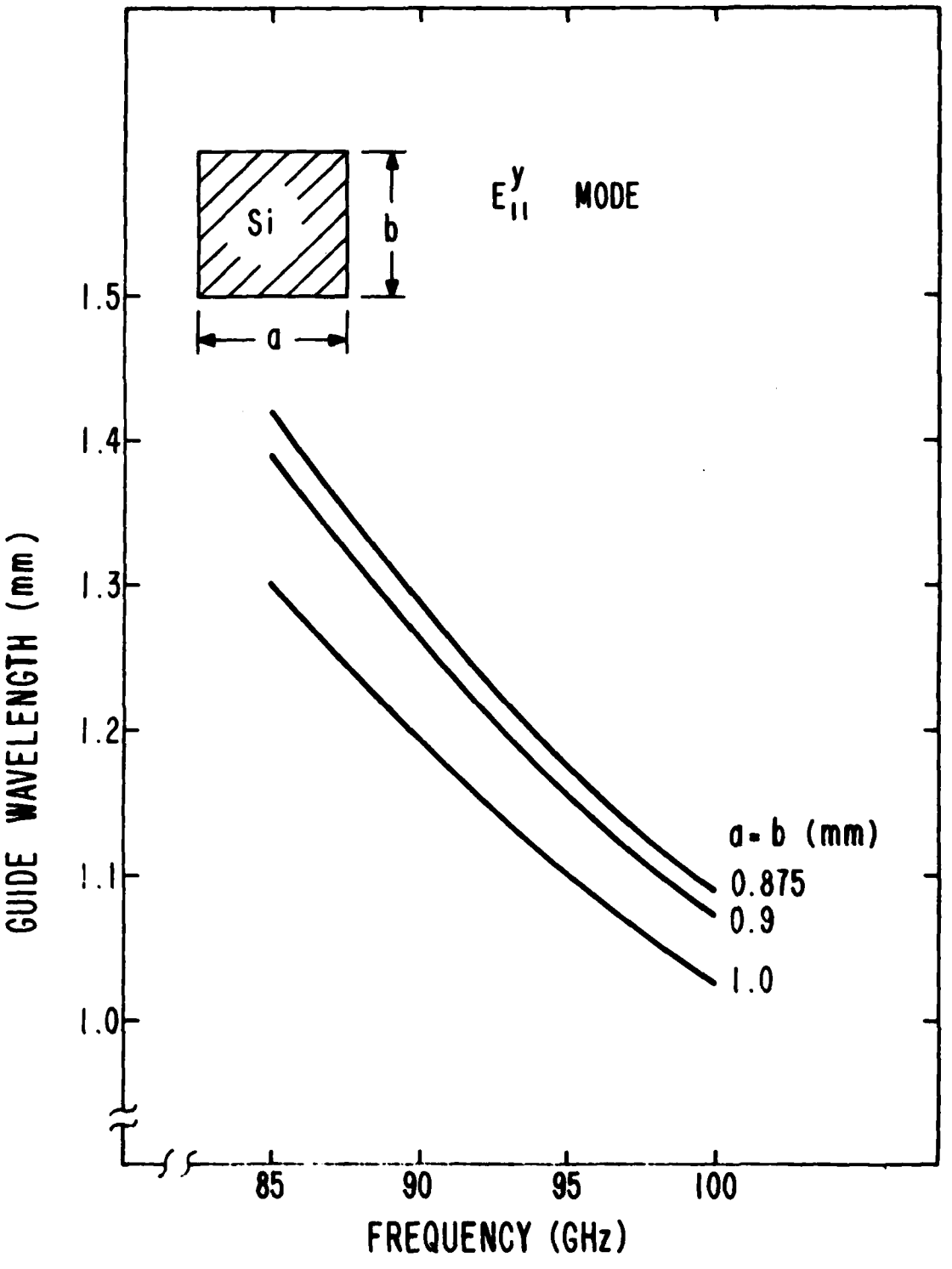

Figure 5 Variation in Guide Wavelength with Frequency as a Function of Size

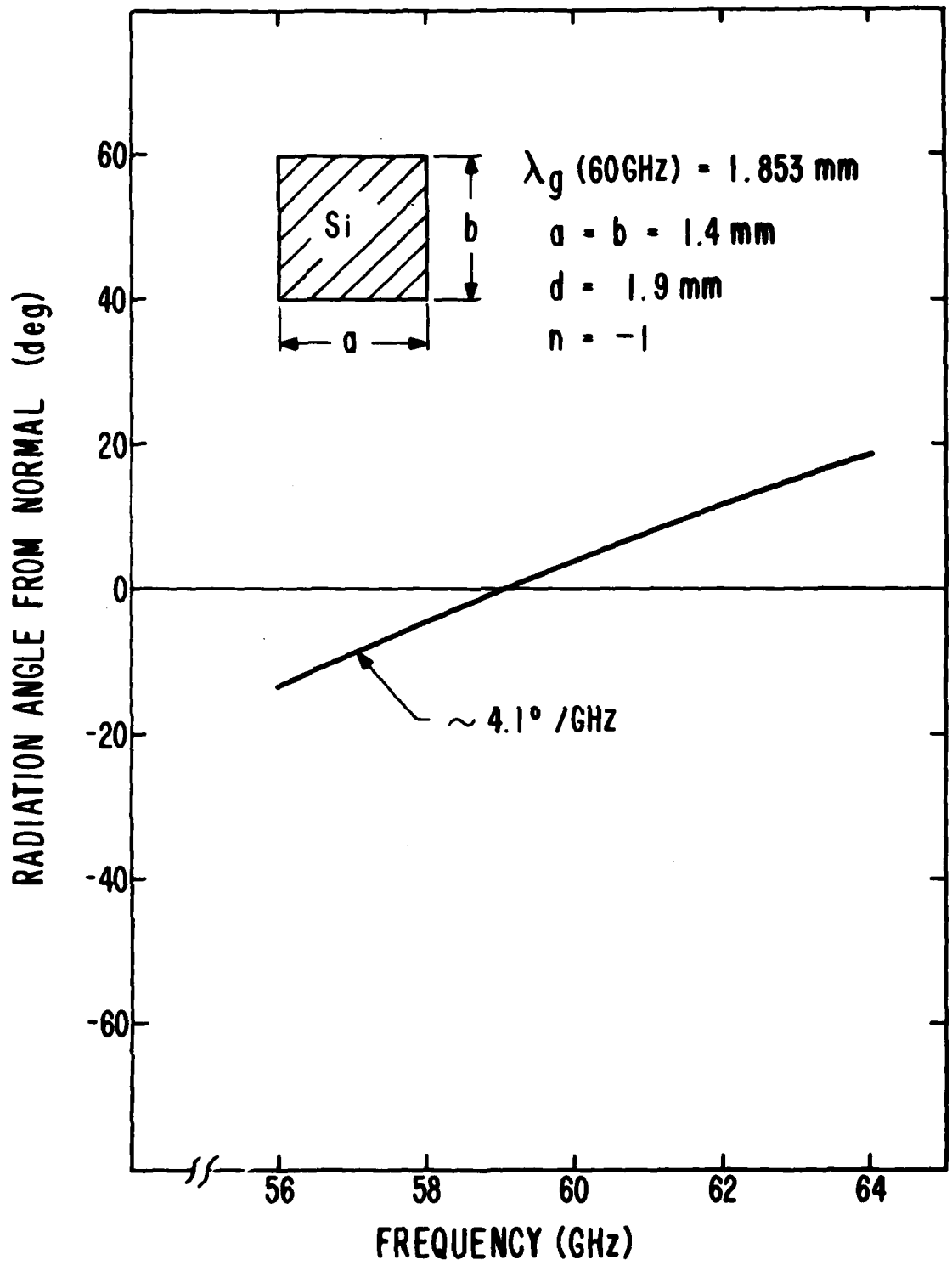

Figure 6 Radiation Angle versus Frequency (60 GHz Design Frequency)

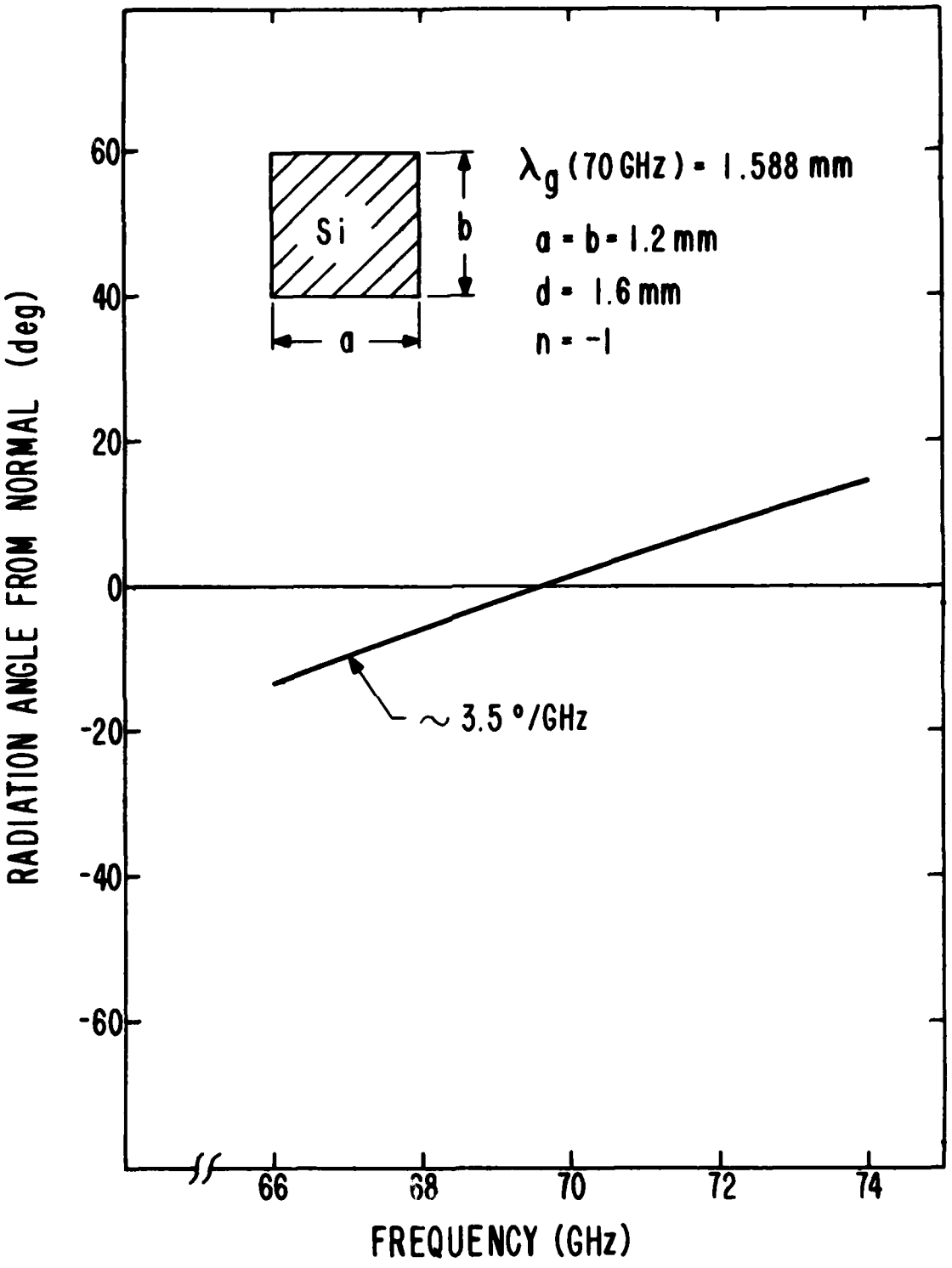

Figure 7 Radiation Angle versus Frequency (70 GHz Design Frequency)

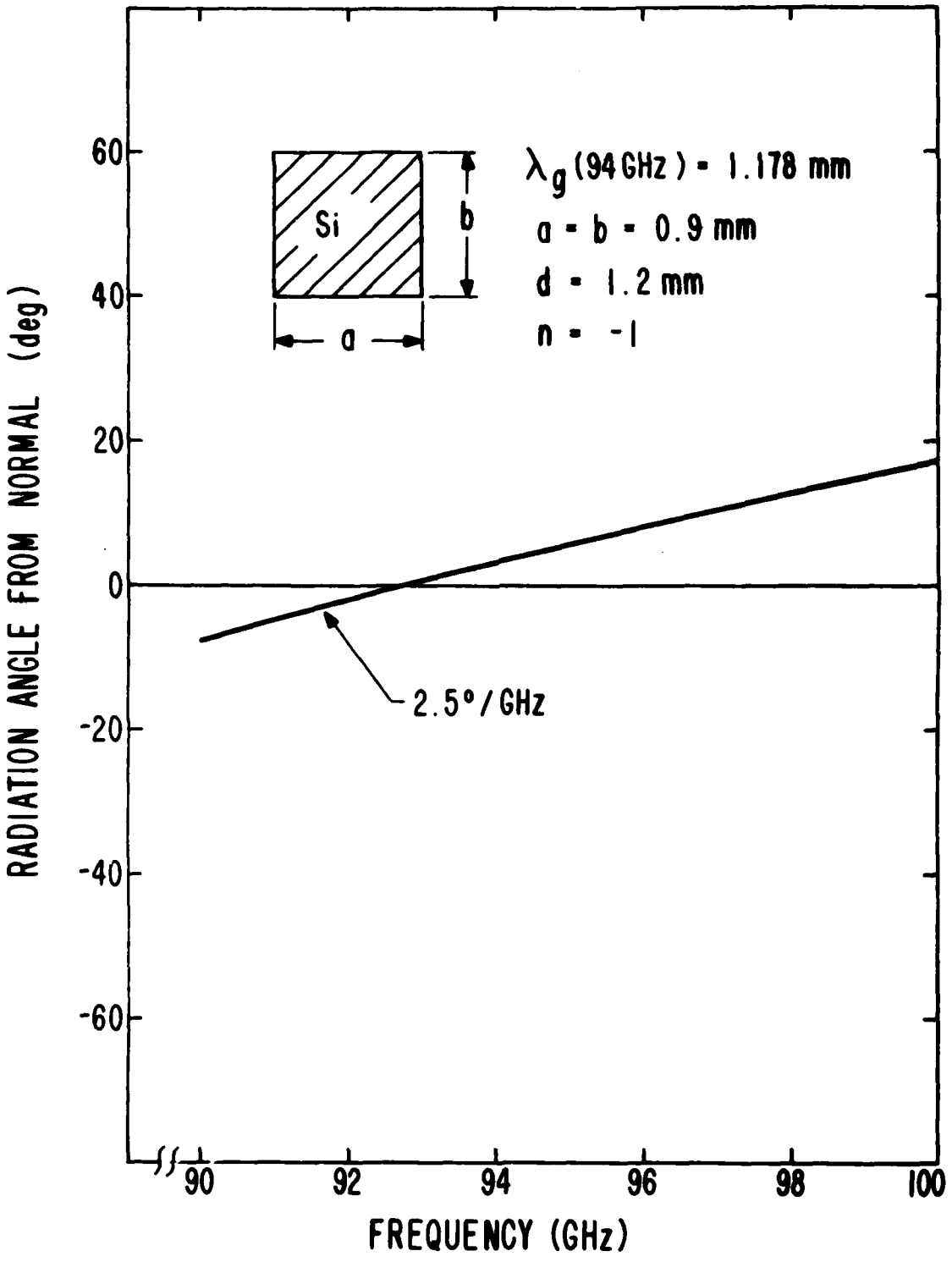

Figure 8 Radiation Angle versus Frequency (94 GHz Design Frequency)

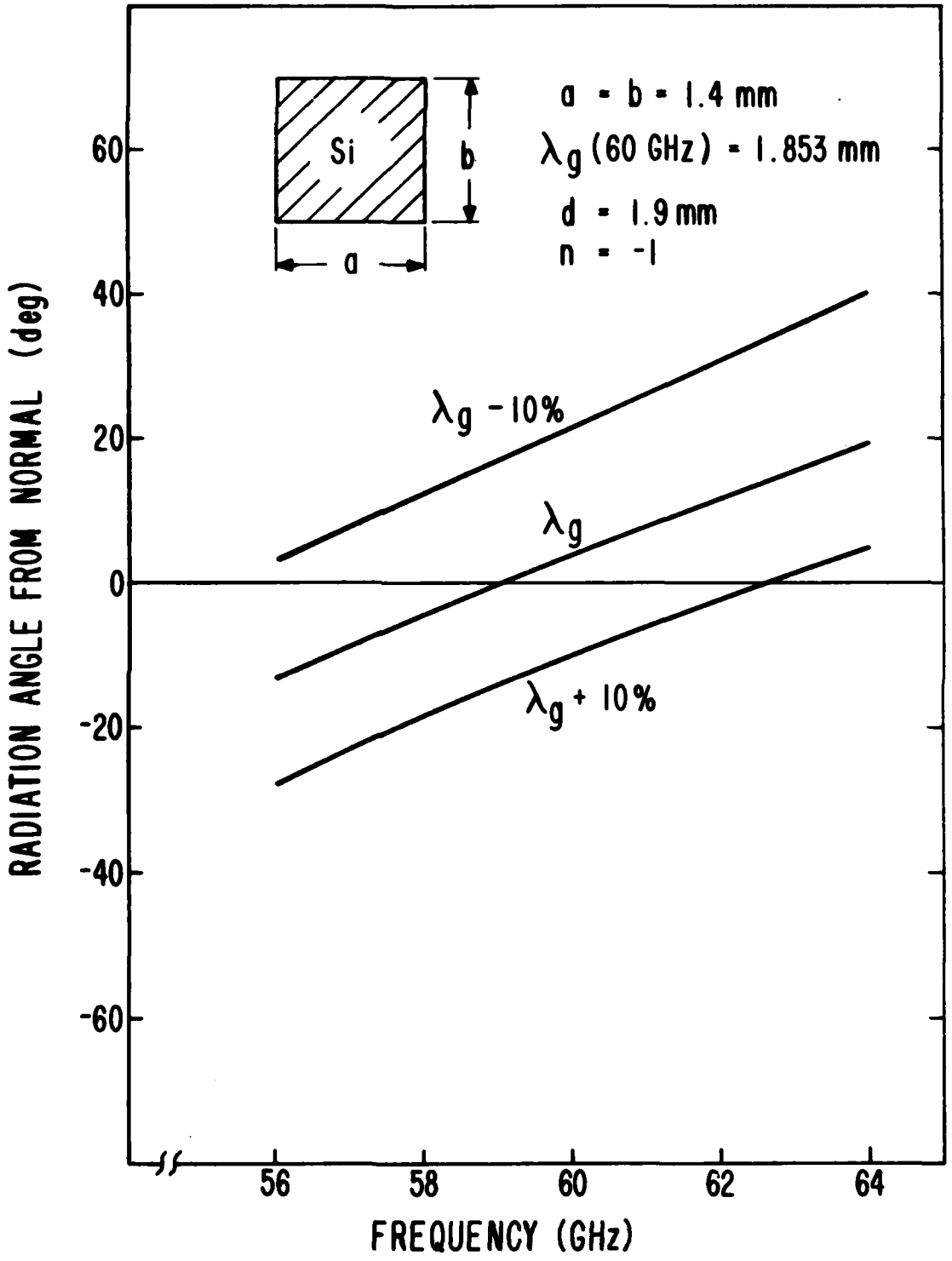

Figure 9 Effect of λ_g on Radiation Angle

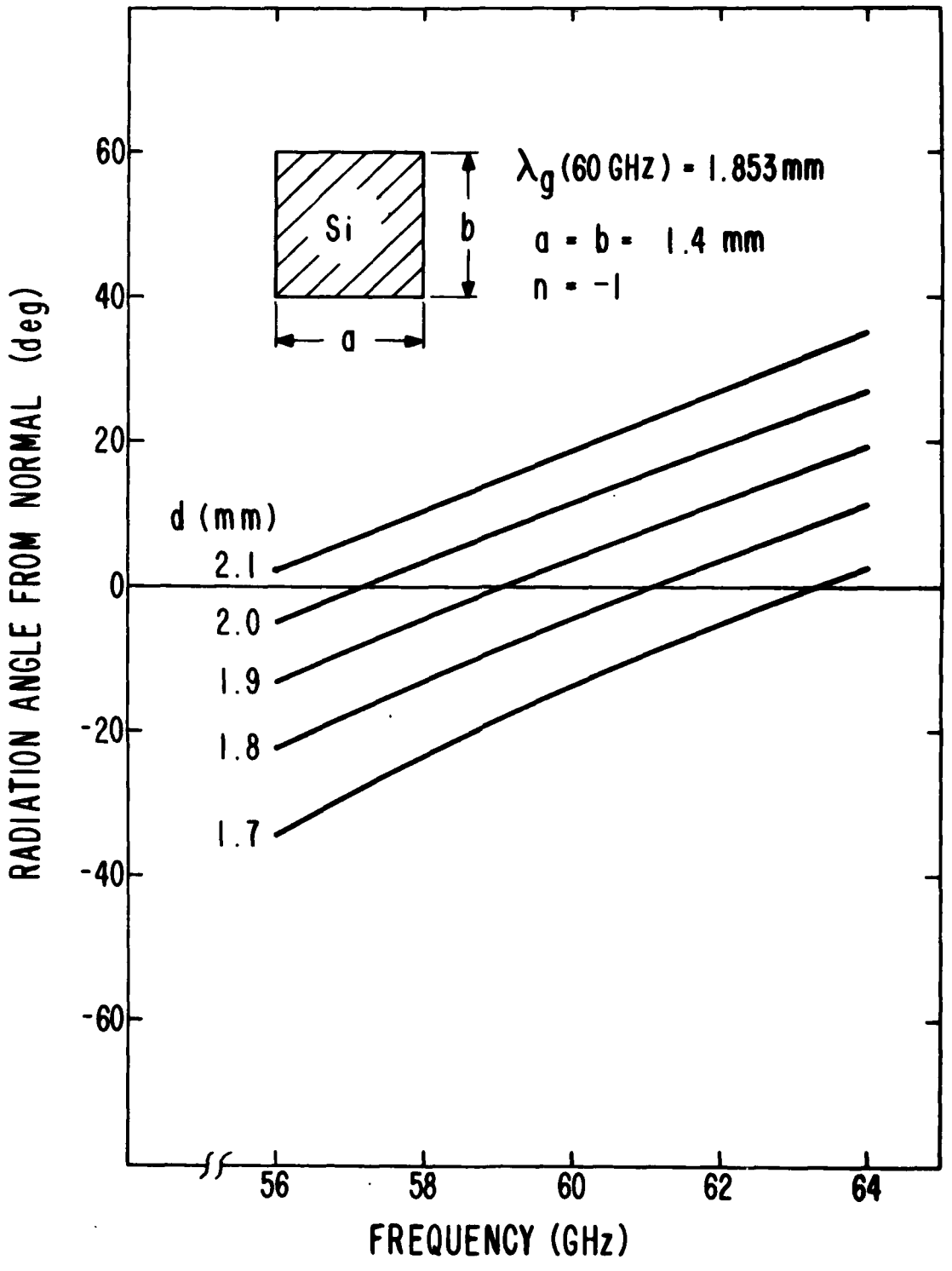

Figure 10 Effect of Perturbation Spacing d on Radiation Angle

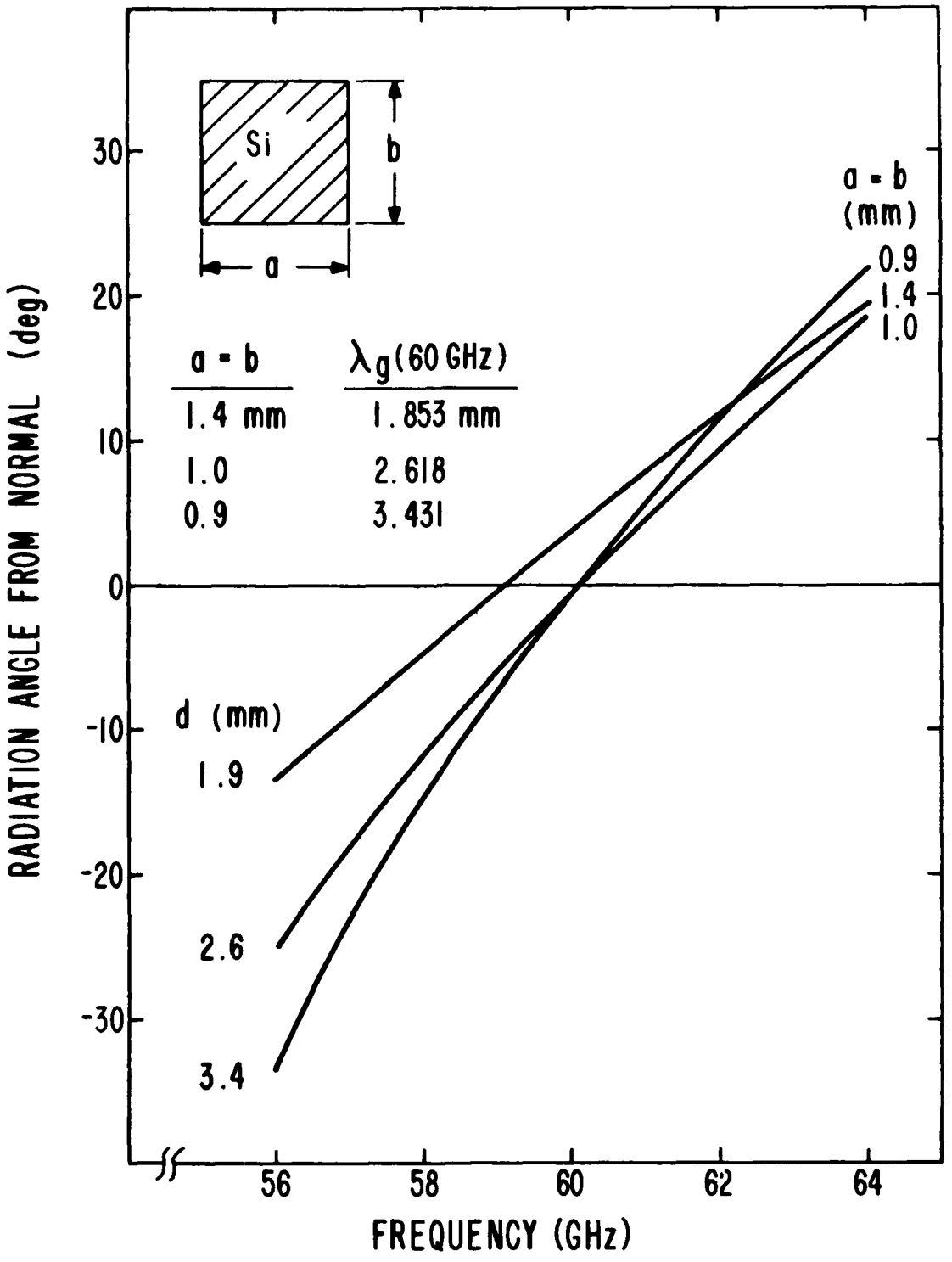

Figure 11 Effect of Guide Size on Angular Scan with $d \approx \lambda_g$ at 60 GHz Design Frequency

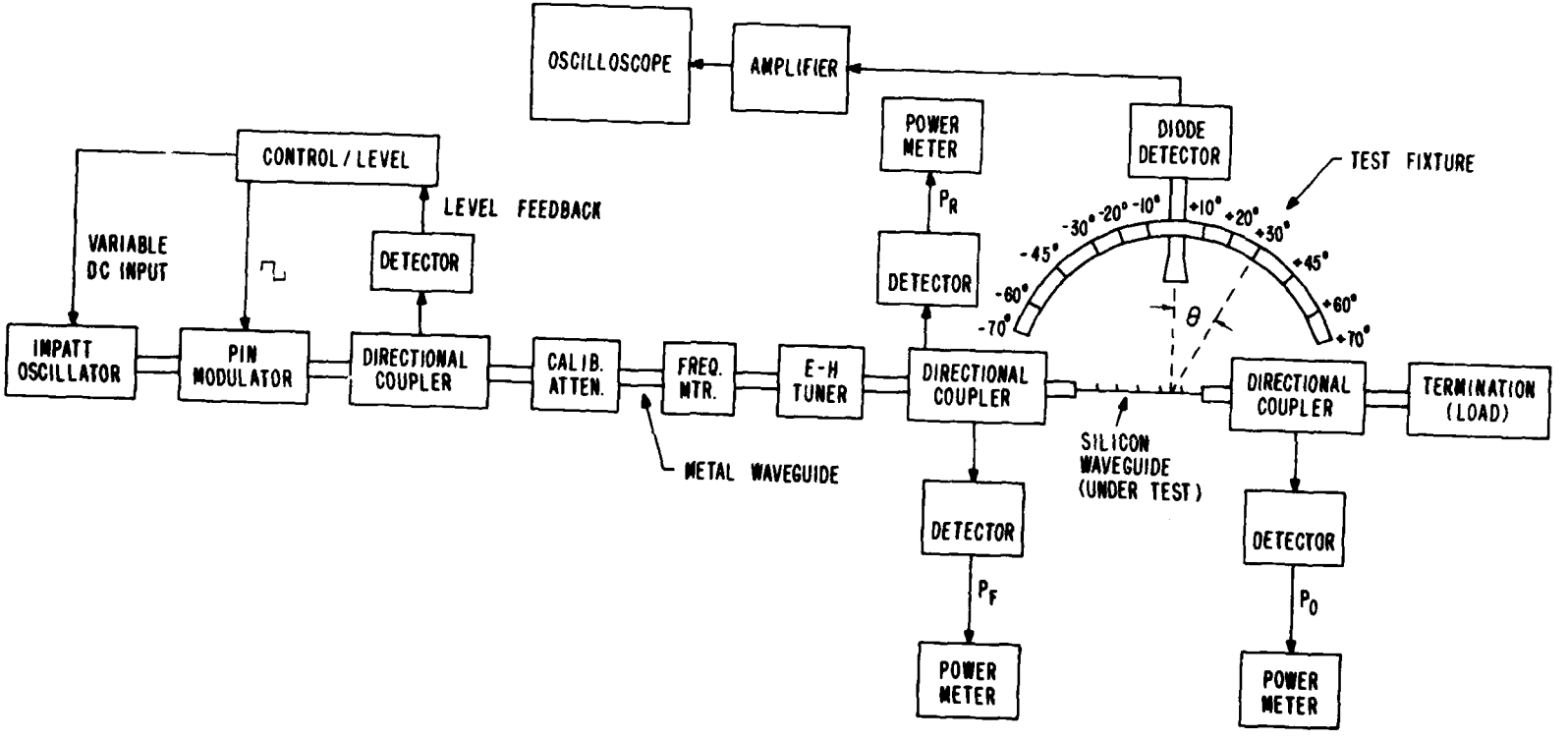

Figure 12 Test Setup for Measurement of Radiation Angle θ versus Frequency

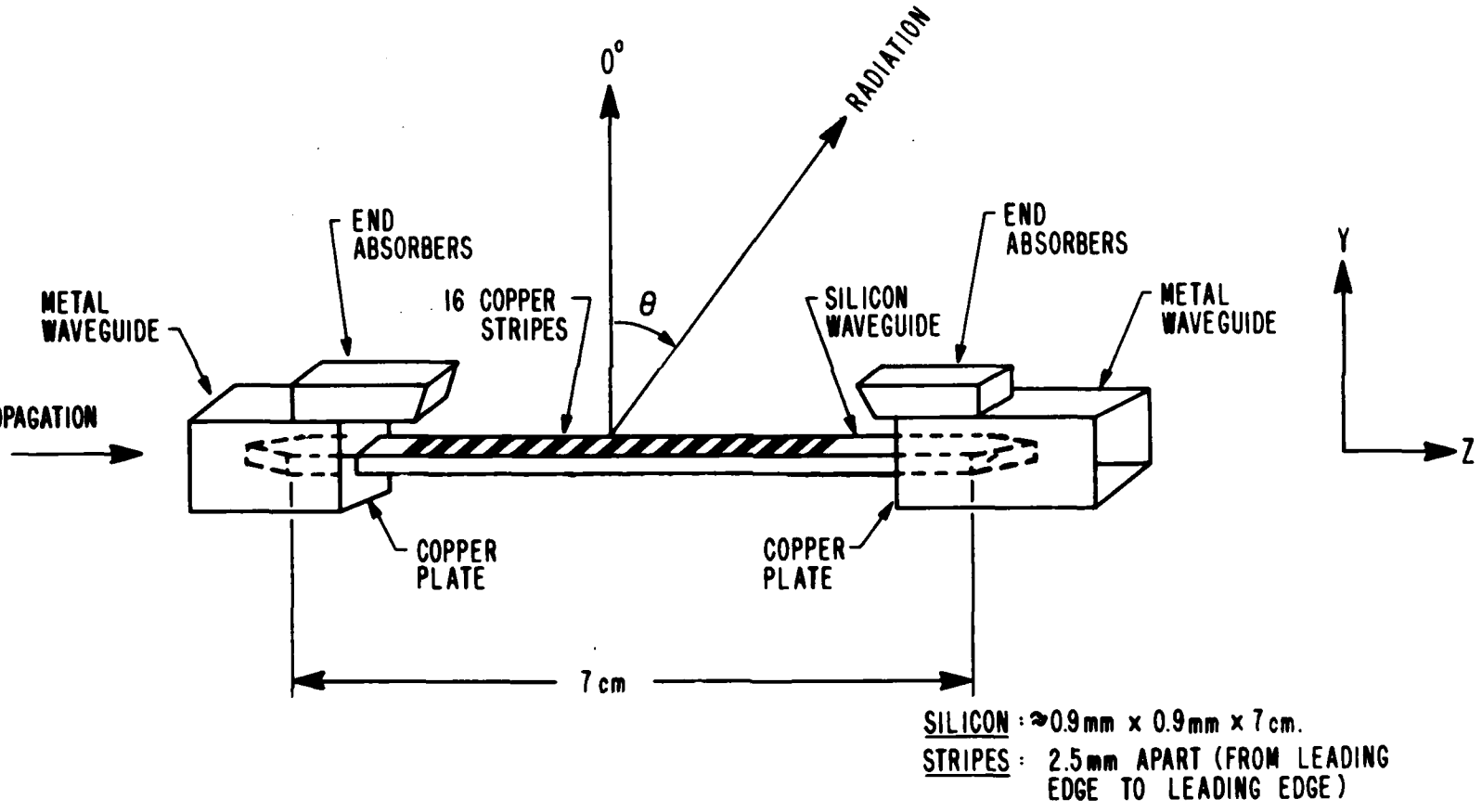

Figure 13 Silicon Waveguide with Perturbations

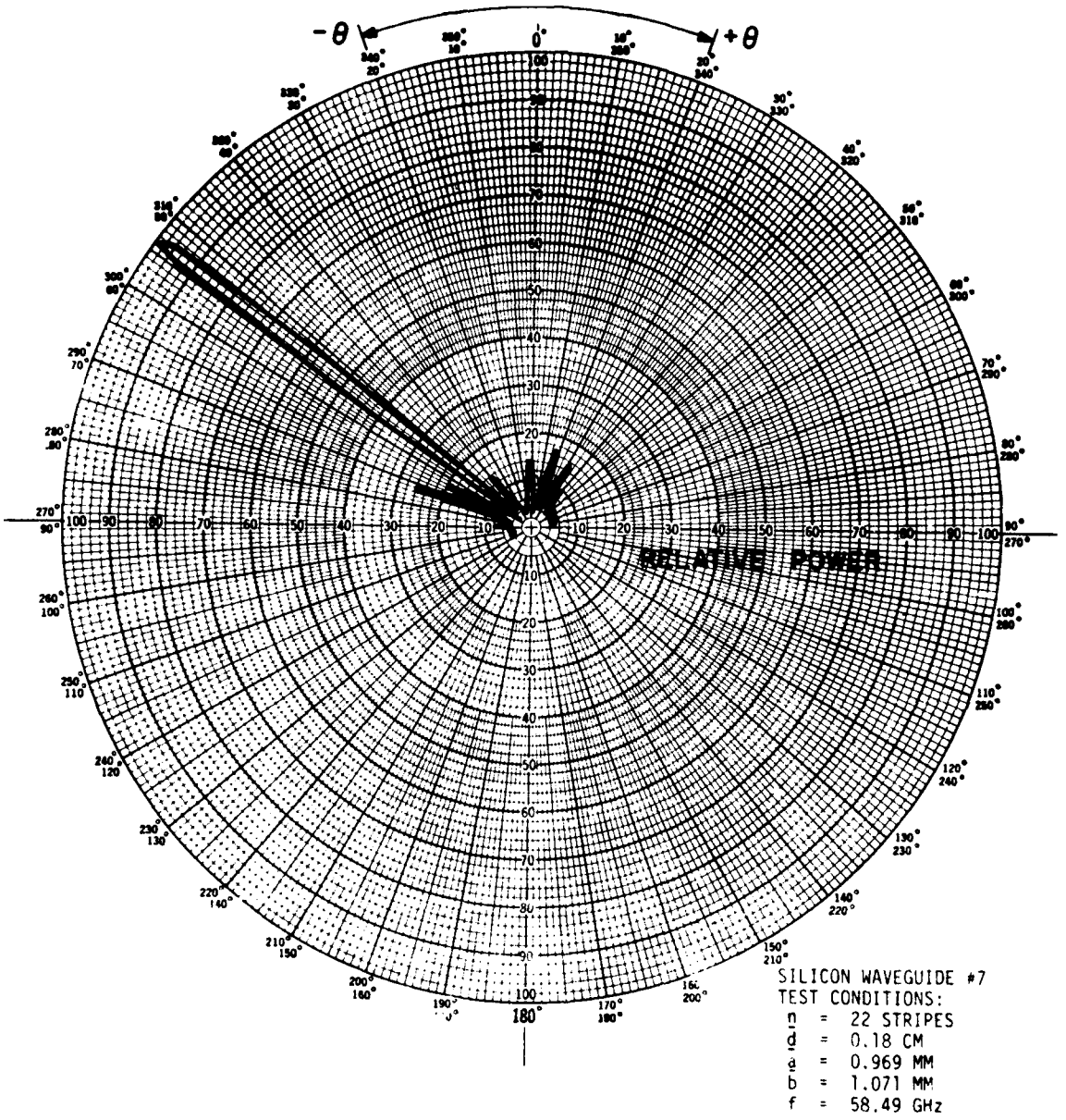

Figure 14a Polar Plot of Beam Angle
y-z Plane

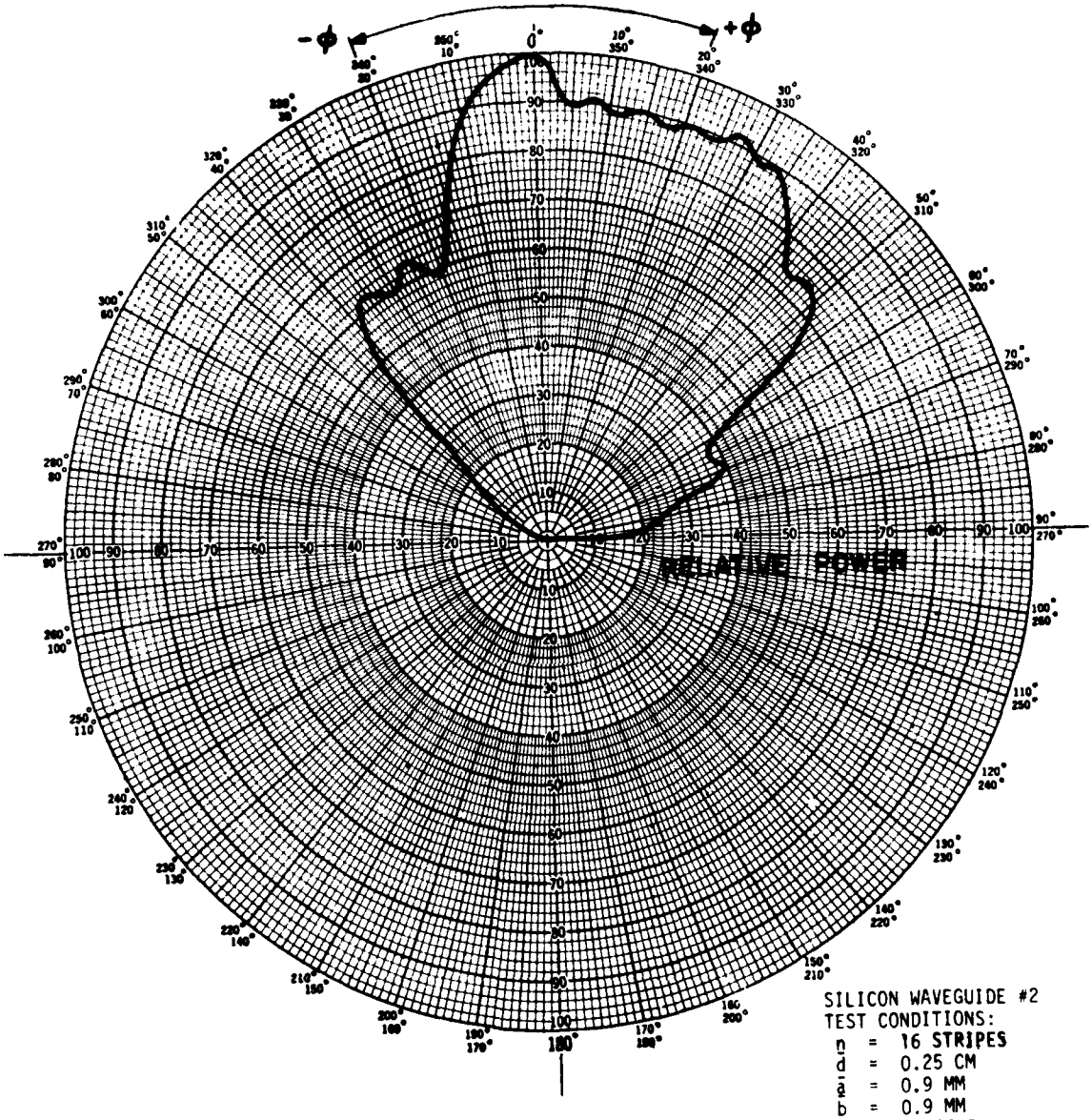

Figure 14b Polar Plot of Beam Angle
r-ϕ Plane

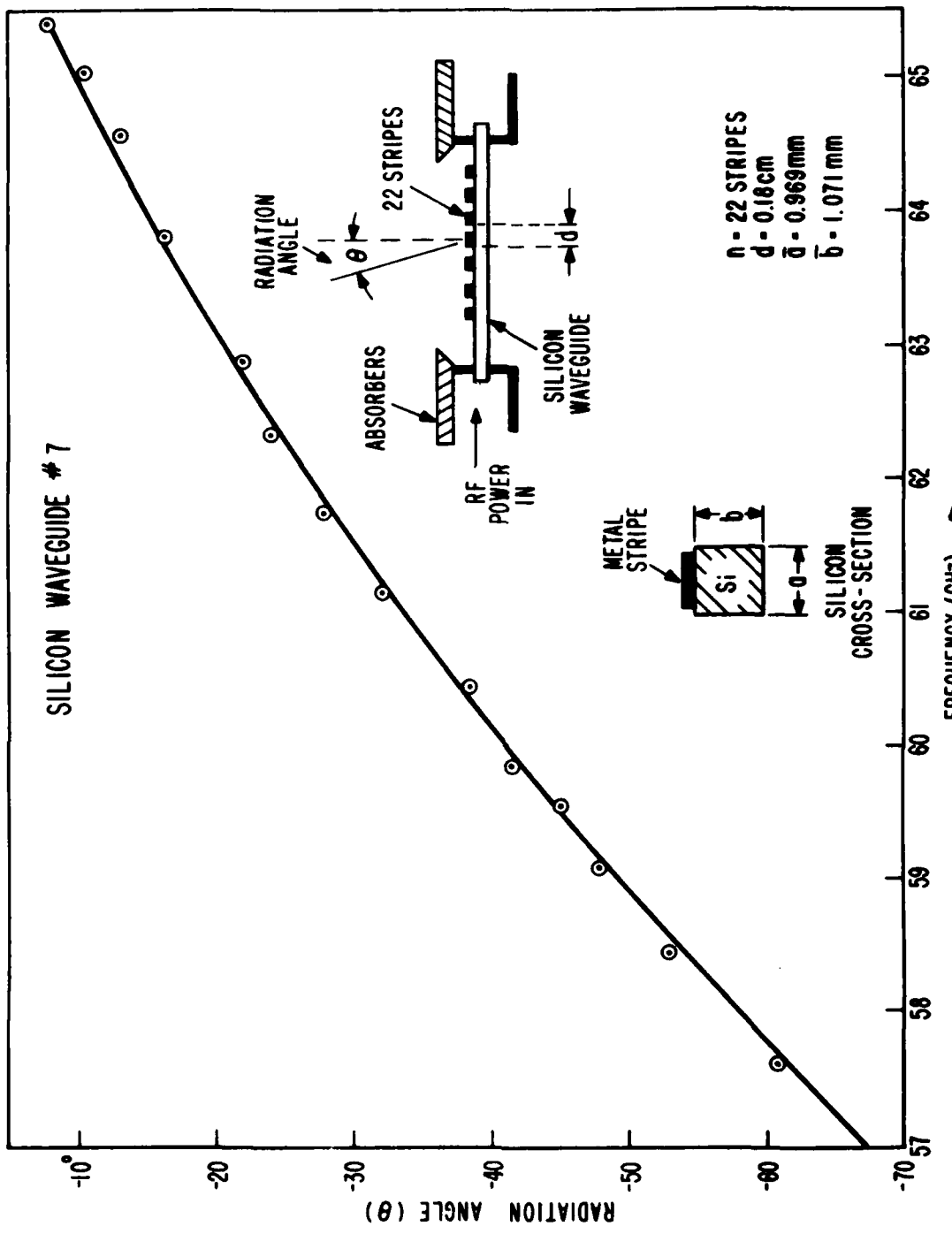

Figure 15 Experimental Plot of Radiation Angle versus Frequency

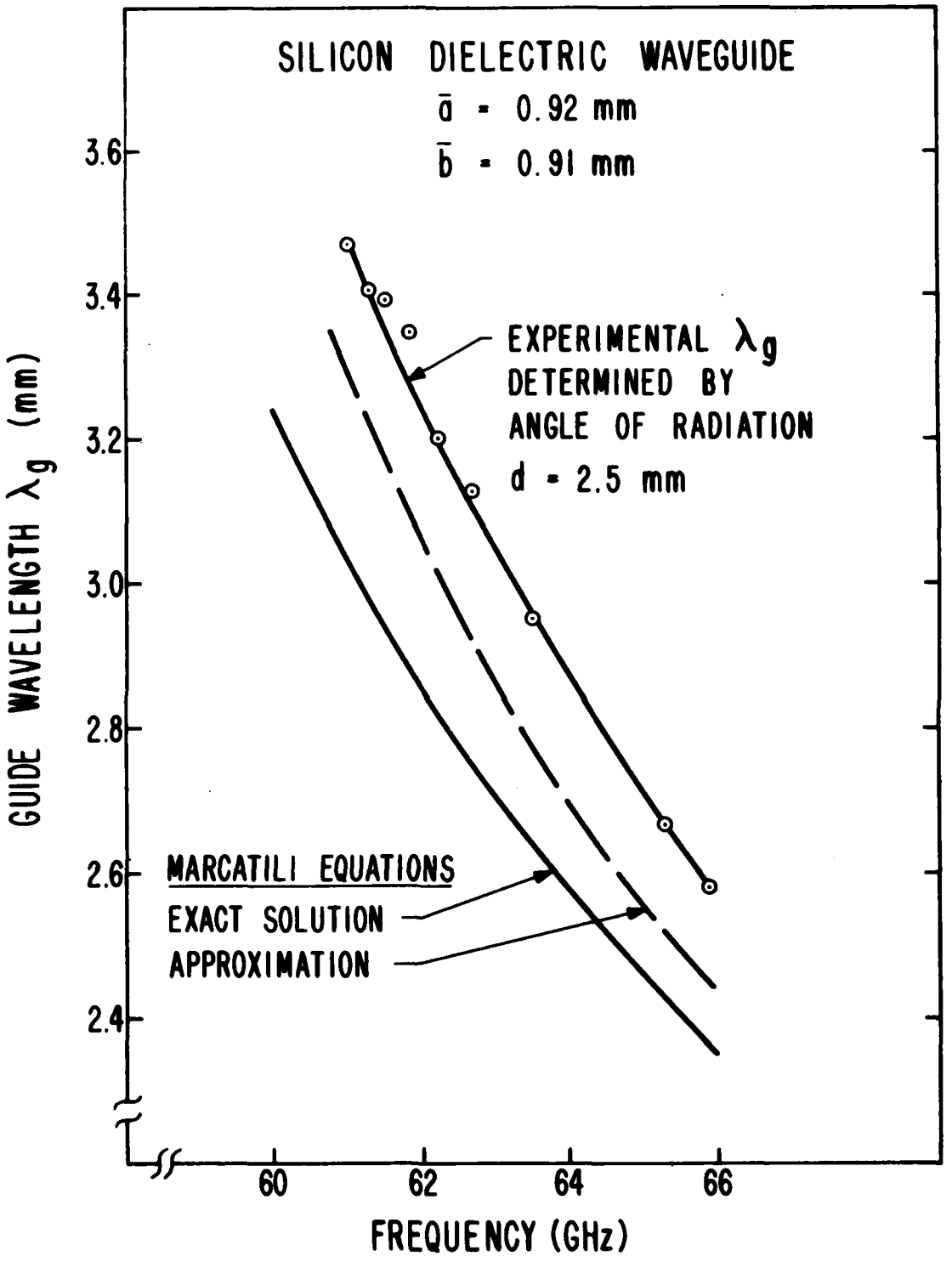

Figure 16 Comparison of λ_g Obtained Experimentally from the Radiation Angle with Theory

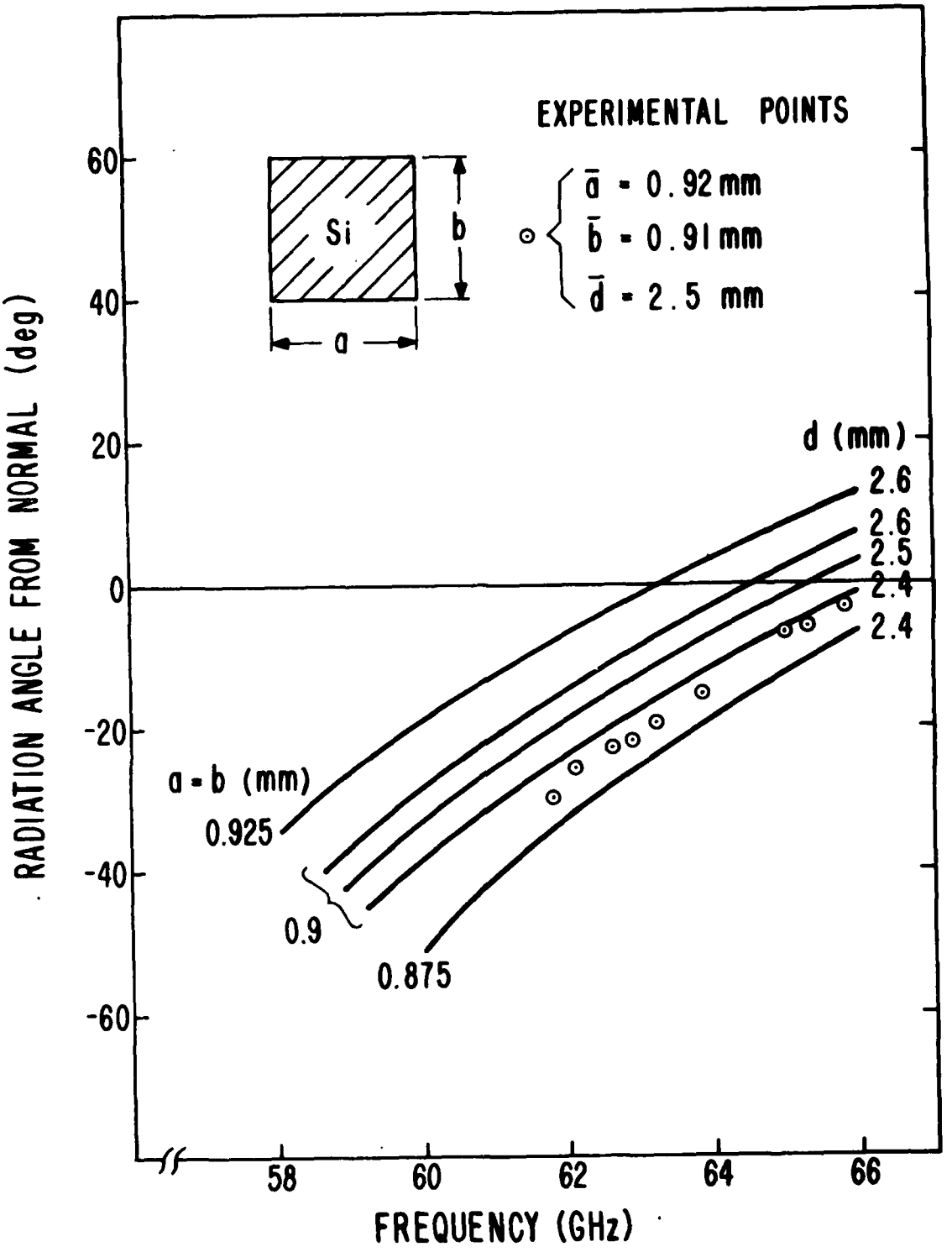

Figure 17a Comparison of Theory and Experiment for Radiation Angle versus Frequency for Various Guide Sizes and Perturbation Spacings

(Silicon Waveguide # 2)

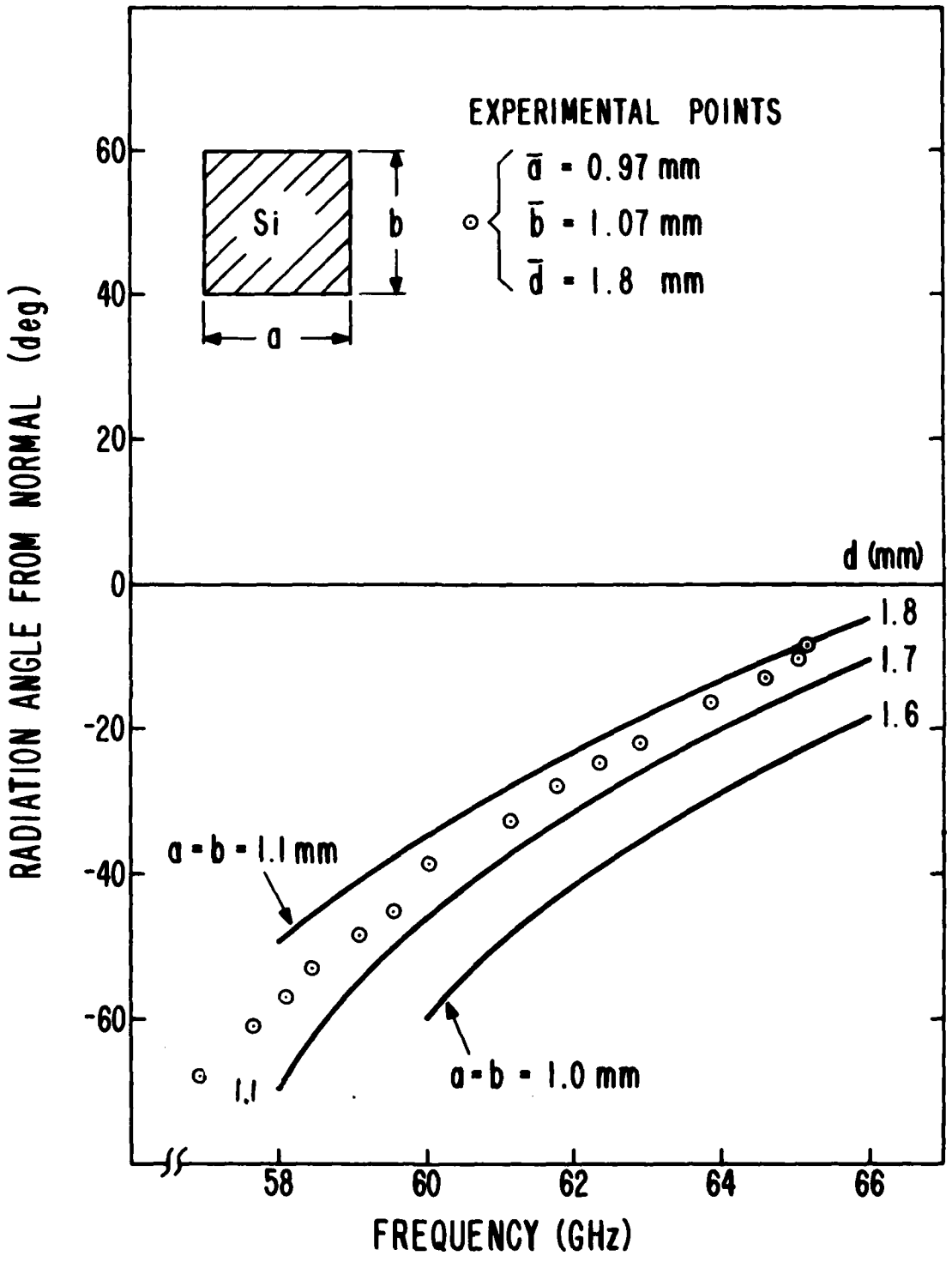

Figure 17b Comparison of Theory and Experiment for Radiation Angle versus Frequency for Various Guide Sizes and Perturbation spacings

(Silicon Waveguide # 7)

APPENDIX A

Calculation of Transverse Propagation Constants in Dielectric Waveguides

The mathematical equations which contain the transmission properties of a rectangular dielectric waveguide relate to the situation shown in Figure A1. The index of refraction n_1 for medium 1, (silicon) is larger than that of the surrounding media (air) n_2, n_3, n_4, and n_5. If $n_2=n_3=n_4=n_5$, the field distributions will be symmetrical about the x and y planes as illustrated. Marcatili [1] developed the following basic equations:

$$k_1 = \frac{2\pi}{\lambda_o} n_1 = 2\pi f \sqrt{\mu_1 \epsilon_1} \qquad [A1]$$

and

$$k_z = \sqrt{k_1^2 - k_x^2 - k_y^2} \qquad [A2]$$

where k_1= propagation constant in medium 1, k_z= axial propagation constant, k_x, k_y = transverse propagation constants in x,y direction, $\mu_1=\mu_r\mu_o$= permeability of medium 1, (μ_r=1 for Si), $\epsilon_1 = \epsilon_r \epsilon_o$ = permittivity of medium 1 (ϵ_r=12 for Si). The transverse propagation constants k_x and k_y are solutions of the transcendental equations,

$$k_x a = p\pi - \tan^{-1}(k_x \xi_3) - \tan^{-1}(k_x \xi_5) \qquad [A3]$$

$$k_y b = q\pi - \tan^{-1}\left(\frac{n_2^2}{n_1^2} k_y \eta_2\right) - \tan\left(\frac{n_4^2}{n_1^2} k_y \eta_4\right) \qquad [A4]$$

where a equals the x dimension (width) and b equals the y dimension (height) of the silicon waveguide and

$$\xi_{3,5} = \frac{1}{\sqrt{\left(\frac{\pi}{A_{3,5}}\right)^2 - k_x^2}} \qquad [A5]$$

$$\eta_{2,4} = \frac{1}{\sqrt{\left(\frac{\pi}{A_{2,4}}\right)^2 - k_y^2}} \qquad [A6]$$

where

$$A_{2,3,4,5} = \frac{\lambda_o}{2\sqrt{n_1^2 - n_{2,3,4,5}^2}} \qquad [A7]$$

1. E.A.J. Marcatili, "Dielectric Rectangular Waveguide and Directional Coupler for Integrated Optics", Bell System Technical Journal, Vol 48, No. 7, September 1969.

The number of extrema contained within the guide in the x and y directions are indicated by p and q, respectively. For the fundamental E^y_{11} mode, both p and q equal one. Figure A1 illustrates that $\xi_{3,5}$ and $\eta_{2,4}$ are the distances the fields penetrate the respective surrounding mediums. $A_{2,3,4,5}$ indicate the maximum physical dimensions of the waveguide which will support only the fundamental mode provided the guide is surrounded by a uniform medium of equal refractive index. Equations [A3] and [A4] were solved exactly using a programmed calculator [2] by plotting the right and left hand sides of each equation for a range of k_x and k_y values, respectively. The exact numerical values for k_x and k_y at the point of intersection (right hand side of the equation equal to left hand side) was determined by employing the "coarse grid approach" [3] to search for the minimum difference between the two curves for each equation.

Approximations

If the approximations of Equation [4] are used, based on the fact that for well-guided modes most of the power will travel within medium 1, and the fact that the arctan and the argument of a small angle are approximately equal, Equations [A3] and [A4] can be simplified to,

$$k_x = \frac{p\pi}{a}\left(1 + \frac{A_3 + A_5}{\pi a}\right)^{-1} \qquad [A8]$$

$$k_y = \frac{q\pi}{b}\left(1 + \frac{n_2^2 A_2 + n_4^2 A_4}{\pi n_1^2 b}\right)^{-1} \qquad [A9]$$

These equations can then be readily solved for k_x and k_y and the guide wavelength calculated using Equation [A2] and

$$\lambda_g \equiv \lambda_z = 2\pi / k_z \qquad [A10]$$

The agreement between λ_g (exact) and λ_g (approximate) improves as the wavelength becomes smaller with respect to the cross-sectional dimensions of the guide. This also means that more of the electric field stays within the waveguide boundaries.

2. K.L. Klohn, J.F. Armata, Jr., and M.M. Chrepta, "Transverse Propagation Constants in Dielectric Waveguides", R&D Technical Report ECOM-4242, US Army Electronics Command, Fort Monmouth, N.J., August 1974.
3. G. L. Neuhauser, Introduction to Dynamic Programming, John Wiley and Sons, Inc., New York, N.Y., 1967, pp 104-111.

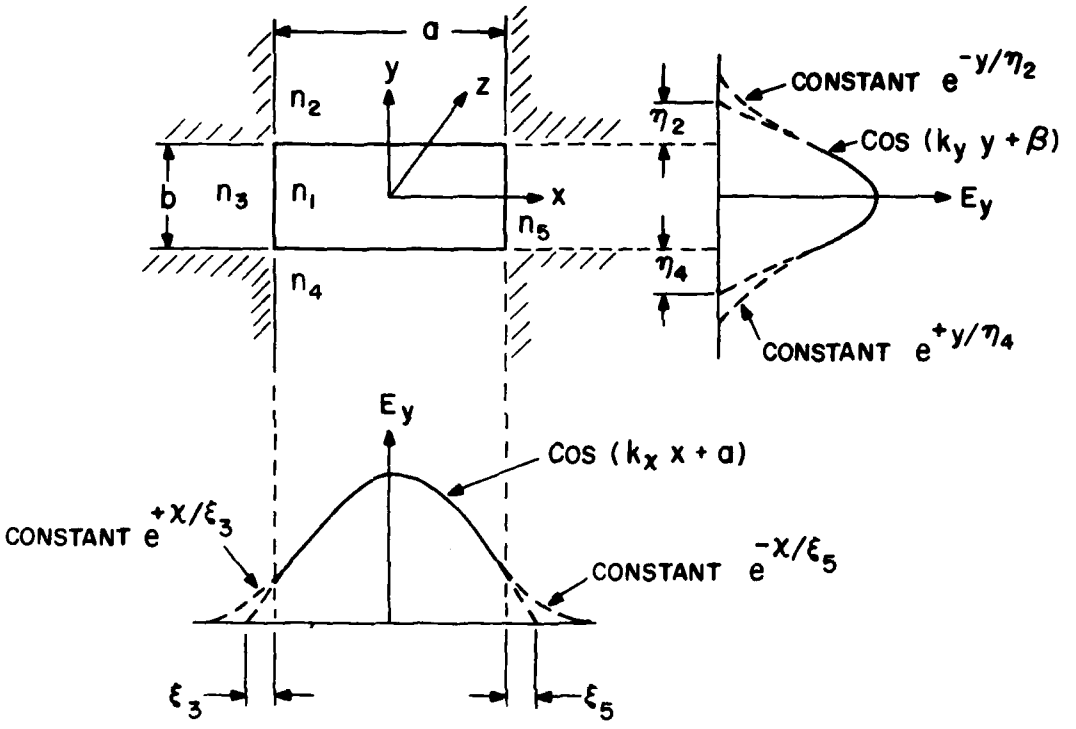

Figure A1 Silicon Waveguide n_1, Immersed in Air, $n_2=n_3=n_4=n_5=1$